

Operating a PbWO₄ EM calorimeter in a harsh radiation environment

Marta Tornago^{1,*} on behalf of the CMS Collaboration

¹CEA Paris-Saclay, DPhP/IRFU

Abstract. The CMS Electromagnetic Calorimeter (ECAL) is the largest homogeneous calorimeter operating in a high energy physics experiment. During the course of the LHC Run 1, Run 2, and Run 3, ECAL has made essential contributions to the CMS physics program by precisely measuring the energy, position, and time of arrival of photons and electrons, and of hadronic jets. Among the masterpieces of physics results achieved with its excellent energy resolution is the observation of the Higgs boson in its two photon decay in 2012, and the precise measurement of its properties.

Operating a lead-tungstate scintillating calorimeter to such high precision and in a harsh radiation environment requires full control of the environmental conditions, such as temperature and bias voltages of the photodetectors, and a continuous correction of the crystal response changes. This paper focuses on the challenges faced over the recent Run 3 years – experiencing the largest instantaneous luminosity up to now – and describes the calibration techniques developed and the achieved results, also including the evolution of the monitoring system in preparation of the High Luminosity phase of the LHC.

1 Introduction

The Electromagnetic Calorimeter (ECAL) [1] of the Compact Muon Solenoid (CMS) [2] is the largest homogeneous calorimeter operating in a high energy physics experiment. Its purpose is to measure the energy, position, and time of arrival of photons and electrons. It contributes to the measurements of hadronic jets and missing transverse energy (MET). ECAL includes 75848 lead-tungstate PbWO₄ crystals: 61200 are arranged in 36 supermodules in the barrel region, while the remaining 14648 equip the four half-disks of the two endcaps. The ECAL barrel covers the pseudorapidity region $|\eta| < 1.48$ and the endcaps cover $1.48 < |\eta| < 3$. Scintillation light produced in the crystals is read out by Avalanche Photodiodes (APDs) in the barrel and Vacuum Phototriodes (VPTs) in the endcaps. In front of the ECAL endcaps, a preshower detector, consisting of two double-layered disks made of lead and silicon strips, helps distinguish single photons from photons from π^0 decays.

The CMS ECAL aims to achieve an excellent energy resolution throughout the LHC operations. The resolution measured during Run 2 for high quality (low Bremsstrahlung) electrons from Z decays – with energy between 35 and 80 GeV – ranges between 1.7% and 3% for $|\eta| < 1.48$ and is $\sim 4\%$ for $1.48 < |\eta| < 2.5$ [3, 4]. The design of the calorimeter has been optimized for the quest for the Higgs boson –then discovered– focusing on its decay into two photons. ECAL has made essential contributions to the CMS physics program during the course of the LHC Run 1, Run 2, and Run 3.

2 ECAL operations during LHC Run 3

The calorimeter is currently running in CMS, taking part in the operations of the LHC Run 3, which started in 2022 and will extend until the end of 2025. The total integrated luminosity recorded by CMS since the start of the LHC operations is $\sim 250 \text{ fb}^{-1}$, with a peak luminosity of $2 \times 10^{34} \text{ cm}^{-2}\text{s}^{-1}$ reached during Run 2. The last years of Run 3 experience the largest luminosity ($2.6 \times 10^{34} \text{ cm}^{-2}\text{s}^{-1}$), with a mean pileup (simultaneous proton-proton interactions) of 46 and 52 in 2022 and 2023 respectively [5]. During Run 3 the L1 trigger rate increased from the 100 kHz of Run 2 to 110 kHz in 2023. [6].

The high pile-up and trigger rate of Run 3 represent a challenging environment for ECAL operations. In order to collect high-quality data and operate ECAL reliably in harsh conditions, it is fundamental to carefully supervise the detector operations, and create a strong synergy among ECAL data acquisition, trigger, detector safety and control, and electronics. During Run 2 ECAL operations, thanks to an optimized control of hardware, software and environmental conditions, 98% of the channels were operational and the luminosity loss caused by ECAL was limited to about 0.3% of the total luminosity, corresponding to about 8% of the total luminosity loss of CMS.

The same number of operational channels has been maintained also during Run 3. The luminosity lost by ECAL is maintained around 8% of the CMS total, despite the increased pileup and rate, thanks to the decrease of the downtime duration from 20h and 25 minutes of Run 2 (2016-2018) to 7h and 23 minutes in the first two years of Run 3. ECAL downtimes are mainly caused by Single Event Upsets, whose recovery software has been recently improved with the implementation of automatic ac-

*e-mail: marta.tornago@cern.ch

tions that reduced the recovery time of one event from 30 s in Run 2 to 12 s in Run 3. In addition, the ECAL Detector Control and Safety System has been further improved with the introduction of a new set of automatic actions, alarms, and notifications.

In order to cope with large event size and very high rate—more than what ECAL was originally designed for—zero-suppression thresholds have been adapted to reduce the stress on the ECAL DAQ while avoiding losing data. A demonstration of ECAL capabilities in facing the Run 3 challenges is represented by the 2023 Heavy Ion run. ECAL managed to withstand the large event size of ion collisions keeping an excellent data quality thanks to the optimized zero-suppression settings.

3 ECAL calibration and monitoring

Accurate design and attentive operations are not the only ingredients to achieve high precision in a harsh radiation environment: other key elements are its constant monitoring and calibration [3]. The transparency of the lead-tungstate crystals drifts with time due to crystal defects produced by radiation. While hadronic damage is permanent, electromagnetic-induced defects anneal spontaneously at room temperature, producing a partial recovery of the crystal transparency in the absence of collisions. In order to maintain an excellent energy resolution, each crystal is constantly monitored and its response corrected for variations. Energy in ECAL is measured as the energy of deposits in ECAL barrel and endcap produced by showering in the tracker material:

$$E_{e,\gamma} = GF_{e,\gamma} \sum_i S_i(t) C_i A_i, \quad (1)$$

where $G(\eta)$ is the absolute energy scale (~ 40 (60) MeV per ADC count in EB (EE) at the beginning of operations), $F_{e,\gamma}$ is an energy correction for material effects, and A_i is the pulse amplitude in ADC counts for the channel i . $S_i(t)$ is a correction that accounts for response variations with time, derived by means of a dedicated laser monitoring system. It is computed from the ratio of the initial response to laser light of the crystal R_0 at the start of the first year of data taking to the response at the time t $R(t)$. An intercalibration coefficient C_i is computed for each crystal as a combination of different calibration constants that accounts for the intrinsic differences in individual crystal light-yield and photodetector response. It includes both the channel-to-channel intercalibration and the absolute scale calibration. Prompt feedback on the energy response stability is provided during data taking using methods based on electrons and photons from decays of physics candles, such as Z , W , and π^0 .

In order to guarantee the best possible prompt energy calibration, ECAL needs a weekly update of pedestals, a continuous update of the laser corrections for each crystal, and a fine tuning with residual corrections extracted from physics processes. Prompt calibrations are deployed in offline reconstruction—starting 48h after data taking—for physics analyses. At the trigger level, dedicated calibrations are applied to the online energy reconstruction

performed with fast signal processing. The resulting Trigger Primitives, including a transverse energy measurement for a matrix of crystals and a bit to reject non-scintillation signals, are used to verify that events satisfy the Level-1 trigger requirements [7].

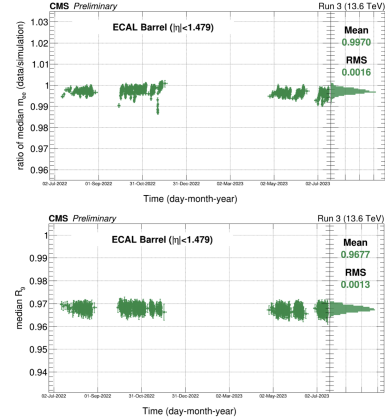


Figure 1. Stability of the di-electron invariant mass comparing data and simulation (top) and stability of the shower shape (bottom) over 2022 and 2023 using $Z \rightarrow e^+e^-$ for ECAL barrel [8].

The large majority of ECAL calibration and reconstruction techniques has been proved to be solid in the Run 2 environment. A framework has been developed to automate the calibration and monitoring workflows, providing simple monitoring tools and optimizing the person-power [9]. The core functionality of the framework has been commissioned between 2021 and 2022, and the workflow integration has been performed during 2022 and 2023. The framework has worked reliably during 2023. All workflows for ECAL calibration are already in production, and the framework has been successfully adopted also by other CMS subsystems. An example of physics validation performed by the automated framework is the stability over time of reference measurements, such as:

- the di-electron invariant mass m_{ee} from Z decays (Fig. 1, top);
- the shower shape of electromagnetic deposits using $Z \rightarrow e^+e^-$ (Fig. 1, bottom). It is represented by $R_9 = E_{seed}/E_{3 \times 3}$, ratio between the energy of the crystal with the largest deposit (seed) and the total energy collected in the 3×3 matrix built around it. R_9 depends on energy intercalibration, noise, and pileup, and allows to distinguish between high and low quality (low and high Bremsstrahlung) electrons (using a threshold value $R_9^{Thr} = 0.965$).

Among the well-established calibration techniques, the energy intercalibration based on the $Z \rightarrow e^+e^-$ channel can benefit from a high statistics during Run 3. The channel intercalibration computed for 2022 and 2023 with Z peak show a good stability over the whole 2022-2023 period despite the luminosity increase and the detector ageing. intercalibrations with π^0 and W decays are also available for future improvements.

Changes in the crystals transparency are constantly mon-

itored and corrected by a laser monitoring system [10]. Light from a laser source is sent to each crystal with a multi-level system of optical fibres and a two-level distribution system on detector. The same light is sent simultaneously to reference PN diodes, readout by an electronic chain specifically designed. A blue (447 nm) and a green (527 nm) laser continuously sweep all ECAL, and provide a measurement of the response for each crystal every ~ 40 minutes (Fig. 2). The measurements are used to apply quasi-real-time corrections to the data, within 48h from the data taking, in time for the CMS data reconstruction. Measurements from the laser monitoring system allow the derivation of correction factors for energy measurements for each crystal at the trigger level. The frequency of the update of trigger-level corrections was once per week at the beginning of Run 2, and increased up to once per fill in Run 3, accounting for the higher beam intensities.

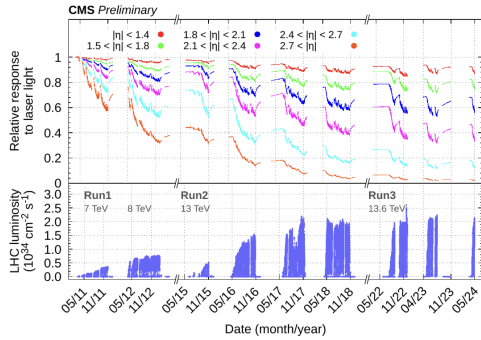


Figure 2. Relative response to laser light from 2011 for different ECAL η regions (top) with the corresponding instantaneous luminosity (bottom) [8].

The laser room was recently relocated from the underground service cavern to surface to make space for the installation of the cooling system of the Endcap Timing Layer and the High Granularity Calorimeter, that will instrument the CMS experiment during the High-Luminosity LHC. A pilot run of the new laser room was performed in June 2023 with a spare laser and its controller on surface. The stability of laser pulse shapes has been verified, and the change in shape with the additional extra 150 m fibres was proven to be negligible. The amplitude of laser pulses decreases by a factor ~ 2 in 100 m (3 dB/100 m), compensated with an increase of the laser power. The laboratory has been completely relocated on surface in November 2023, during the End-of-Year Technical Stop, and successfully commissioned. The new laboratory complies with the requirements of a temperature stability of $\pm 0.3^\circ\text{C}$ and a relative humidity $< 40\%$, ensuring the stability of the laser pulse and timing. Timing stability allows the laser to be issued in the dedicated 25-ns calibration window in the LHC abort gap, i.e. the empty segment of the LHC orbit. The system has been operational since the CMS restart in 2024, and is ready for the High-Luminosity era (see Sect. 5). The data taking during the commissioning in November 2023 allowed the laser system precision to be verified after the relocation. Results show a precision $< 6 \times 10^{-4}$ in the barrel and up to

10^{-3} in the endcaps, well within requirements (2×10^{-3}) and comparable with 2011 results considering the signal-to-noise ratio reduction [8].

In addition, the new laser room has been equipped with a new more powerful green laser (Photonics DP20-B527). The upgrade of the laser sources will permit facing the transparency loss that the ECAL endcaps will experience during Run 3, especially in the regions with the highest pseudorapidity and in the last years of data taking. The commissioning was completed at the beginning of 2024 and the new green laser is currently running in place of the legacy green.

ECAL also provides information on the arrival time of electrons and photons, which is particularly relevant e.g. to study long lived particles characterized by a delayed signature. For timing reconstruction, the default algorithm in Run 2 and 2022-2023 data reconstruction was the Ratio Timing. This algorithm determines the pulse timing relative to the time of the maximum amplitude from a reference template exploiting the ratio between consecutive samples $A(t)$ and $A(t+25\text{ ns})$ [3]. A new Cross-Correlation (CC) algorithm has been developed and tested during Run 2 [11]. CC timing associates a templated pulse shape with each out of time (OOT) amplitude, subtracts the OOT pulses from the measured pulse to extract the in-time one, and finds the time that best matches the signal pulse to the templated pulse shape with a cross correlation fit. The new algorithm includes rejection of non-scintillation signals and OOT pileup awareness, and allows a significant improvement in time resolution both in Run 2 and Run 3 data (35 ps improvement in Run 2 data for $Z \rightarrow e^+e^-$, with electrons p_T peaking at ~ 35 GeV). It is currently being commissioned.

The timing measurement –which assumes a fixed pulse shape– is affected by the evolution of crystal pulse shapes in time, due to changes in transparency under irradiation. Timing calibrations based on physics candles are applied on daily basis to obtain the final timing measurement, and allow to reduce the variation in clock distribution between different ECAL regions and different CMS runs.

4 ECAL performance

ECAL energy resolution is computed with $Z \rightarrow e^+e^-$. The stability of m_{ee} over time in Fig. 1 is observed at 0.1% level throughout 2022 and 2023, bringing to a stable energy resolution. Energy resolution in Run 3 for Low (High) Bremsstrahlung electrons is 1.5% (2.4%) in ECAL barrel and 3% (3.6%) in the endcaps. A slight loss of performance is observed with respect to Run 2 due to increased pileup (Fig. 3). Studies are ongoing to further improve the Run 3 algorithms for clustering the energy deposits of electrons and photons in the ECAL. A new method has been developed based on deep neural networks [12]. Unlike the current method [13], that aggregates crystals within parabolic regions to recover deposits from photon conversions and electron Bremsstrahlung, the new method is a more sophisticated algorithm built with graph neural networks that first aggregate crystals in clusters and then clusters together. Clusters close to the highest energy one

are grouped together and analyzed by a Machine Learning model to predict their association and reconstruct the supercluster. This method is more resilient to noise and pileup contamination and can be also exploited to distinguish between jets and electromagnetic showers. Simulations show that Deep Neural Network SuperClustering allows an improvement of energy resolution for high energy electrons –especially at $1 < |\eta| < 1.5$, where more secondary deposits are produced due to the higher material budget in front of ECAL– and for photons, which produce fewer secondary deposits. In addition, results prove that the resolution is independent of the pileup. An overall $\sim 10\%$ improvement is observed with respect to the current method, and it still present after applying energy regression to correct for biases in the measured energy due to pileup or losses in the detector.

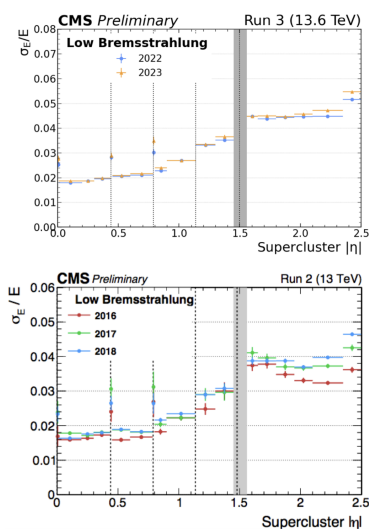


Figure 3. Relative energy resolution versus pseudorapidity for Run 3 (top) and Run 2 (bottom) data [4, 8].

5 ECAL upgrade for High-Luminosity LHC

The Electromagnetic Calorimeter will undergo significant upgrades for the CMS Phase-II during the High Luminosity era of the LHC (HL-LHC) [14], when the luminosity will increase by about a factor 3 with respect to Run 3. The trigger rate will increase from the current 100 kHz up to 750 kHz, with a latency increase from $4 \mu\text{s}$ to $12.5 \mu\text{s}$. To cope with the new demanding conditions, ECAL will need to improve the discrimination of non-scintillation signal and provide an excellent time resolution. To this end, the ECAL barrel electronics will be completely refurbished. The laser monitoring system will be upgraded to have increased redundancy and to be compatible with the refurbished ECAL electronics and the new data acquisition system for CMS.

6 Conclusions

The CMS Electromagnetic Calorimeter (ECAL) is the largest electromagnetic homogeneous calorimeter in high

energy physics and is essential in the CMS physics program thanks to its excellent measurements of energy, position, and time of arrival of photons and electrons, and of jets and MET. During Run 3, operated at record luminosities, ECAL maintained its performance thanks to improvements in operations efficiency. Solid Run 2 algorithms and calibrations have been automated, the laser room of the monitoring system has been relocated on surface to prepare for HL-LHC, and new tools for reconstructing the energy and arrival time of electrons and photons have been developed. This strategy has allowed ECAL to maintain its Run 2 performance in 2022-2023 data.

References

- [1] CMS collaboration, The Electromagnetic Calorimeter Project: Technical Design Report. CERN-LHCC-97-033 (1997).
- [2] CMS Collaboration, The CMS experiment at the CERN LHC. JINST 3 S08004 (2008).
- [3] CMS collaboration, Performance of the CMS electromagnetic calorimeter in pp collisions at $\sqrt{s} = 13 \text{ TeV}$. CERN-EP-2024-014 (2024).
- [4] CMS Collaboration, ECAL 2016 refined calibration and Run2 summary plots. CMS-DP-2020-021 (2020).
- [5] CMS Collaboration, CMS Luminosity - Public results. <https://twiki.cern.ch/twiki/bin/view/CMSPublic/LumiPublicResults>
- [6] E. Yigitbasi for the CMS Collaboration, New CMS trigger strategies for the Run 3 of the LHC. CMS-CR-2023/211 (2023).
- [7] A. Tishelman Charny for the CMS Collaboration, ECAL trigger performance in Run 2 and improvements for Run 3. J. Phys.: Conf. Ser. 2374 (2022).
- [8] CMS Collaboration, ECAL calibration performance in Run 3 with reprocessed data. CMS-DP-2024-022 (2024).
- [9] S. Pigazzini for the CMS Collaboration, Automatic data processing for prompt calibration of the CMS ECAL. CMS-CR-2023/021 (2023).
- [10] M. Anfreville et al., Laser monitoring system for the CMS lead tungstate crystal calorimeter. Nucl. Instrum. Meth. A 594 (2008).
- [11] J. Wang for the CMS Collaboration, Obtaining the ultimate calibration and performance of the CMS Electromagnetic Calorimeter in LHC Run 2. CMS-CR-2023/219 (2023).
- [12] D. Valsecchi for the CMS collaboration, Optimizing electron and photon reconstruction using deep learning application to the CMS electromagnetic calorimeter. CMS-CR-2023/039 (2023).
- [13] CMS Collaboration, Electron and photon reconstruction and identification with the CMS experiment at the CERN LHC. JINST 16 P05014 (2021).
- [14] CMS collaboration, The Phase-2 Upgrade of the CMS Barrel Calorimeters. CERN-LHCC-2017-011 (2017).

